Mon. Not. R. Astron. Soc. **375**, 1315–1324 (2007) doi:10.1111/j.1365-2966.2006.11388.x

White dwarf mass distribution in the SDSS

S. O. Kepler,[1]★ S. J. Kleinman,[2] A. Nitta,[3] D. Koester,[4] B. G. Castanheira,[1] O. Giovannini,[5] A. F. M. Costa[1] and L. Althaus[6]

[1] *Instituto de Física, Universidade Federal do Rio Grande do Sul, 91501-900 Porto-Alegre, RS, Brazil*
[2] *Subaru Telescope, 650 N. A'Ohoku Place, Hilo, HI 96720, USA*
[3] *Gemini Observatory, Hilo, HI 96720, USA*
[4] *Institut für Theoretische Physik und Astrophysik, Universität Kiel, 24098 Kiel, Germany*
[5] *Universidade de Caxias do Sul, 95070-560 Caxias do Sul, RS, Brazil*
[6] *Facultad de Ciencias Astronómicas y Geofísicas, Paseo del Bosque S/N, 1900 La Plata, Argentina*

Accepted 2006 December 6. Received 2006 November 22; in original form 2006 August 1

ABSTRACT

We determined masses for the 7167 DA and 507 DB white dwarf stars classified as single and non-magnetic in Data Release 4 of the Sloan Digital Sky Survey (SDSS). We obtained revised $T_{\rm eff}$ and $\log g$ determinations for the most massive stars by fitting the SDSS optical spectra with a synthetic spectra grid derived from model atmospheres extending to $\log g = 10.0$. We also calculate radii from evolutionary models and create volume-corrected mass distributions for our DA and DB samples. The mean mass for the DA stars brighter than $g = 19$ and hotter than $T_{\rm eff} = 12\,000$ K is $\langle \mathcal{M} \rangle_{\rm DA} \simeq 0.593 \pm 0.016\,\mathcal{M}_\odot$. For the 150 DBs brighter than $g = 19$ and hotter than $T_{\rm eff} = 16\,000$ K, we find $\langle \mathcal{M} \rangle_{\rm DB} = 0.711 \pm 0.009\,\mathcal{M}_\odot$. It appears the mean mass for DB white dwarf stars may be significantly larger than that for DAs. We also report the highest mass white dwarf stars ever found, up to $1.33\,\mathcal{M}_\odot$.

Key words: white dwarfs.

1 INTRODUCTION

White dwarf stars are the end product of evolution of all stars with initial masses up to around $9\,\mathcal{M}_\odot$ and their distribution contains information about star formation history and subsequent evolution in our Galaxy. As the most common endpoints of stellar evolution, white dwarf stars account for around 97 per cent of all evolved stars. Considering there has not yet been enough time for any of them to cool down to undetectability, they can also provide independent information about the age of the Galaxy. Through an initial–final mass relation (IFMR), we can also study mass loss throughout the stellar evolution process. Because white dwarf progenitors lose carbon, nitrogen and oxygen at the top of the asymptotic giant branch (AGB), they are significant contributors to the chemical evolution of the Galaxy and possibly an important source of life sustaining chemicals.

Kleinman et al. (2004) published the spectra of 2551 white dwarf stars in the Sloan Digital Sky Survey (SDSS) Data Release 1 (DR1), covering $1360\,\deg^2$. Eisenstein et al. (2006) extended the white dwarf spectroscopic identifications to the SDSS Data Release 4 (DR4) with a total of 9316 white dwarf stars reported, more than doubling the number of spectroscopically identified stars (McCook & Sion 2003). In both works, the authors fit the entire optical spectra from 3900 to 6800 Å to DA and DB grids of synthetic spectra derived from model atmospheres calculated by Detlev Koester, up to $\log g = 9.0$ (in cgs units). Their fits include SDSS imaging photometry and allow for refluxing of the models by a low-order polynomial to incorporate effects of unknown reddening and spectrophotometric errors. The SDSS spectra have a mean g-band signal-to-noise ratio SNR $(g) \approx 13$ for all DAs, and SNR $(g) \approx 21$ for those brighter than $g = 19$.

This large sample of stars with spectroscopic fits gives us a new opportunity to fully explore the white dwarf mass distribution. Understanding the white dwarf mass distribution offers insights into mass loss during stellar evolution, the IFMR and has bearings on close binary star evolution. Our report, as well as many previous studies, detect a substantial fraction of low-mass white dwarf stars that theoretically cannot have evolved as single stars, because the age of the Universe is smaller than their presumed lifetimes on the main sequence.

Kleinman et al. (2004) notice an increase in mean $\log g$ for stars cooler than $T_{\rm eff} = 12\,000$ K, but caution the trend might not be real, indicating a problem in the data or fit technique, instead. The trend has persisted into the larger catalogue of Eisenstein et al. (2006). Madej, Należyty & Althaus (2004) analysed the Kleinman et al. (2004) sample of fits and calculated the corresponding SDSS DR1 pure hydrogen atmosphere (DA) white dwarf mass distribution. As expected from the $\log g$ trend, they found that the mean mass also increased below $T_{\rm eff} = 12\,000$ K. Their table 1 presents all previous mean mass determinations, producing an average of $0.57\,\mathcal{M}_\odot$, and a most populated peak at $0.562\,\mathcal{M}_\odot$ for the 1175 stars hotter than

★E-mail: kepler@if.ufrgs.br

$T_{\rm eff} = 12\,000$ K. They did not study the potentially highest mass stars with $\log g > 9$, because they were limited by the stellar atmosphere fit by Kleinman et al. (2004) which artificially pegged stars near the upper $\log g = 9.0$ boundary to the boundary itself.

The increase in mean masses fitted from optical spectra below $T_{\rm eff} = 12\,000$ K has been seen prior to Kleinman et al. (2004) and has been discussed since Bergeron, Wesemael & Fontaine (1991) and Koester (1991). It is usually dismissed as due to problems in the models: either convection bringing up subsurface He to the atmosphere, increasing the local pressure, or problems with the treatment of the hydrogen level occupation probability. The new larger SDSS data set, however, now gives another opportunity to explore this trend and evaluate its cause.

Most reported white dwarf mass determinations have been derived by comparing the optical spectra with model atmospheres, as with Kleinman et al. (2004) and Eisenstein et al. (2006). For the DA stars, the H7, H8 and H9 lines, in the violet, are the most sensitive to surface gravity because they are produced by electrons at higher energy levels, those most affected by neighbouring atoms. However, these lines are also in the region where the atmospheric extinction is the largest and typical CCD detectors are the least sensitive. As a consequence, most studies used only the line profiles in their fits, avoiding the dependence on often uncertain flux calibrations. The SDSS white dwarf spectra have good flux calibration and acceptable SNR redwards of 4000 Å. The published SDSS catalogue therefore fits the *entire* optical spectrum, and not just the H lines, as has been traditionally done. The rationale for this approach is the good, uniform spectrophotometry and corresponding broadband photometry that can be used in the fits. In addition, a low-level refluxing is allowed to take out large errors in spectrophotometry and any unknown reddening effects.

In this paper, we will compare the measured white dwarf mass distributions from Kleinman et al. (2004) and Eisenstein et al. (2006) with previous determinations and attempt to assess the reason for the observed increase in mass for lower temperatures. We will also explore the observed mean masses and analyse the two different fitting techniques: line profile versus whole spectrum, to see the effects on the resulting mass distributions.

2 DATA AND MODELS

The SDSS imaged the high Galactic latitude sky in five pass bands: *u, g, r, i* and *z*, and obtained spectra from 3800 to 9200 Å with a resolution of ≈1800 using a twin fibre-fed spectrograph (York et al. 2000). Since we are primarily interested in the mass distribution here, we selected only the single DA and DB stars with $\log g - \sigma_{\log g} \geqslant 8.5$ and $\log g + \sigma_{\log g} \leqslant 6.5$ from the Eisenstein et al. (2006) sample and refit them with an expanded grid of models (see below), using the same AUTOFIT routine as in Eisenstein et al. (2006) and thoroughly described in Kleinman et al. (2004). We excluded all stars classified by Eisenstein et al. (2006) as having either a detectable magnetic field or a companion, metal lines, DABs and DBAs.

Our model grid (Finley, Koester & Basri 1997; Koester et al. 2001) is similar to that used by Eisenstein et al. (2006), but extended in $T_{\rm eff}$ and $\log g$ ($100\,000\,{\rm K} \leqslant T_{\rm eff} \leqslant 6000$ K, $10.0 \leqslant \log g \leqslant 5.0$) and denser. We chose the ML2/$\alpha = 0.6$ parametrization for convection as demonstrated by Bergeron et al. (1995) to give internal consistency between temperatures derived in the optical and the ultraviolet, photometry, parallax and with gravitational redshift. ML2 corresponds to the Bohm & Cassinelli (1971) description of the mixing length theory and $\alpha = \ell/\lambda_P$ is the ratio of the mixing length to the pressure scaleheight. The models include the H_2^+ and H_2 quasi-molecular opacities and only Stark (Lemke 1997) and Doppler broadening, so the line profiles are not precise for $T_{\rm eff} < 8500$ K.

Even though Napiwotzki, Green & Saffer (1999) and Liebert, Bergeron & Holberg (2005) discuss the necessity of using non-local thermodynamic equilibrium (NLTE) atmospheres for the stars hotter than 40 000 K, all quoted values are from local thermodynamic equilibrium (LTE) models, as they also show the NLTE corrections are not dominant, and our number of hot stars is small.

To calculate the mass of each star from the $T_{\rm eff}$ and $\log g$ values obtained from our fits, we used the evolutionary models of Wood (1995) and Althaus et al. (2005) with C/O cores up to $\log g = 9.0$, and O/Ne cores for higher gravities, $M_{\rm He} = 10^{-2}\,M_*$ and $M_{\rm H} = 10^{-4}\,M_*$ or $M_{\rm H} = 0$, to estimate stellar radii for DAs and DBs, respectively. The radius is necessary to convert surface gravity to mass.

3 ANALYSIS

Before exploring the mass distributions, we wanted to examine the different fitting techniques used in the available data sets – the traditional line profile technique and the SDSS whole spectrum approach. We therefore simulated spectra with differing SNRs by adding random noise to our models and fit them with our own set of both line profile and whole spectrum fitting routines. Our Monte Carlo simulations show that in the low SNR regime, SNR $\leqslant 50$, fitting the whole spectra and not just the line profiles gives *more* accurate atmospheric parameters, as long as the flux calibration or interstellar reddening uncertainties do not dominate. We estimate an uncertainty of around $\Delta T_{\rm eff} \simeq 500$ K and $\Delta \log g \simeq 0.10$ at SNR = 40 for the whole spectra fitting. For SNR = 20, similar to the average SDSS spectra for $g < 19$, our simulations indicate $\Delta T_{\rm eff} \simeq 750$ K and $\Delta \log g \simeq 0.15$. We do not report in this paper on the mass distribution for the stars fainter than $g = 19$ because their smaller SNR lead to large uncertainties. Our simulations did not indicate systematic trends between the two approaches.

Although Kleinman et al. (2004) and Eisenstein et al. (2006) compared their fits' internal errors by fitting duplicate spectra, they did not display their results as a function of temperature. Kepler et al. (2005) specifically analysed 109 duplicate spectra SDSS DAs with $13\,000 \geqslant T_{\rm eff} \geqslant 10\,000$ K, near the region where the fit $\log g$s start to increase. They showed that the mean fit differences were $\sigma_{T_{\rm eff}} \simeq 300$ K and $\sigma_{\log g} \simeq 0.21$ dex for the same object but different observations. These values are larger than the internal uncertainty of the fits, but in general within 3σ of each other, as in Kleinman et al. (2004) and Eisenstein et al. (2006). We thus conclude that the uncertainties in Eisenstein et al. (2006) are reasonable and can now analyse the results without attributing any noted irregularities to the fitting process.

Kepler et al. (2006), however, compare SDSS spectra with new SNR (g) $\simeq 100$ spectra acquired with Gemini Multi-Object Spectrograph (GMOS) on the Gemini 8-m telescope for four white dwarf stars around $T_{\rm eff} \simeq 12\,000$ K. Their fits suggest that published SDSS optical spectra fits overestimate the mass by $\Delta\mathcal{M} \simeq 0.13\,\mathcal{M}_\odot$, because of the correlation between the derived $T_{\rm eff}$ and $\log g$ – a small increase in $T_{\rm eff}$ can be compensated by a small decrease in $\log g$. In our simulations this discrepancy is concentrated only in the region around the Balmer line maximum, $14\,000 \geqslant T_{\rm eff} \geqslant 11\,000$ K.

To explore the increasing mass trend in more detail, we restricted our sample to the 1733 stars both brighter than $g = 19$ and hotter than $T_{\rm eff} = 12\,000$ K and obtained an average DA mass of $\langle\mathcal{M}\rangle_{\rm DA} = 0.593 \pm 0.016\,\mathcal{M}_\odot$. The distribution for this hot and bright sample, shown in Fig. 1, is similar to that of the Palomar Green survey published by Liebert et al. (2005). They studied a

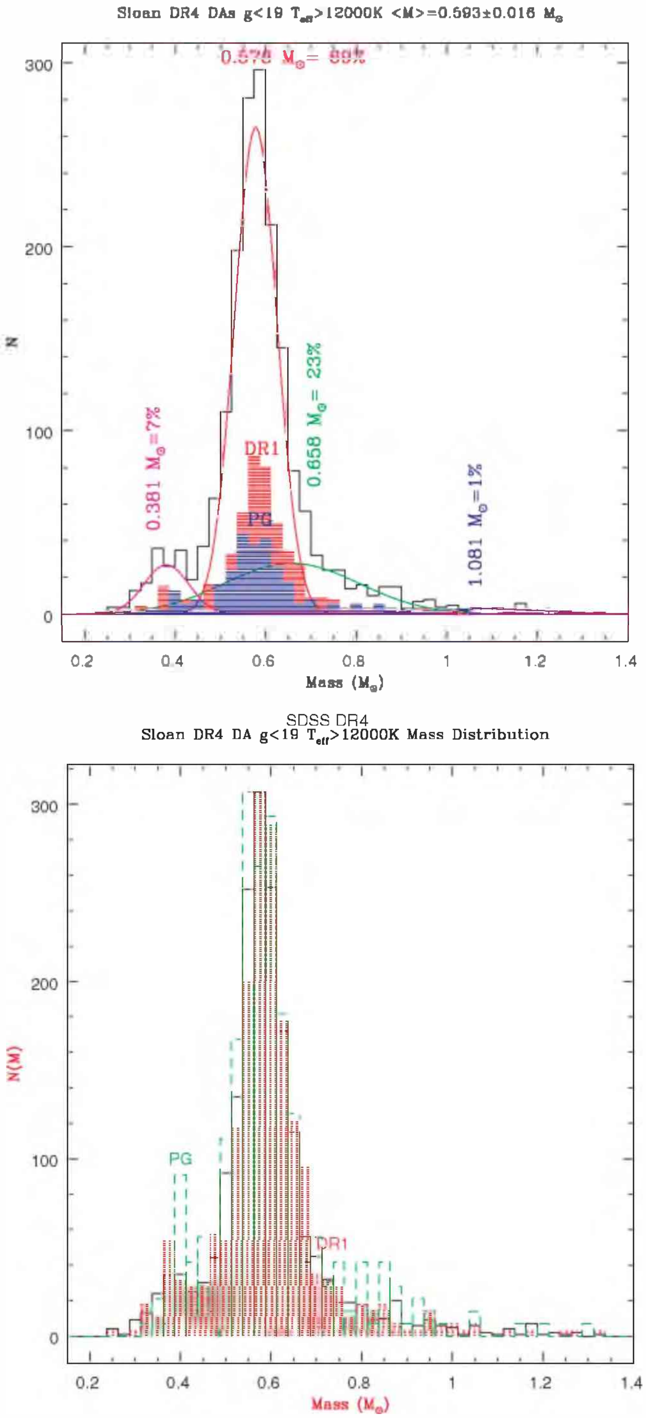

Figure 1. Histogram for the 1859 DA stars brighter than $g = 19$ and hotter than $T_{\rm eff} = 12\,000$ K, compared to the PG survey published by Liebert et al. (2005) and the SDSS DR1 sample published by Madej et al. (2004). Gaussian fits detailed in Table 1 are also shown. Our bins are 0.025-$\mathcal{M}_\odot$ wide. The second graph shows the DR1 and PG survey data normalized to the DR4 sample, even though those samples are smaller and therefore have significantly larger error bars.

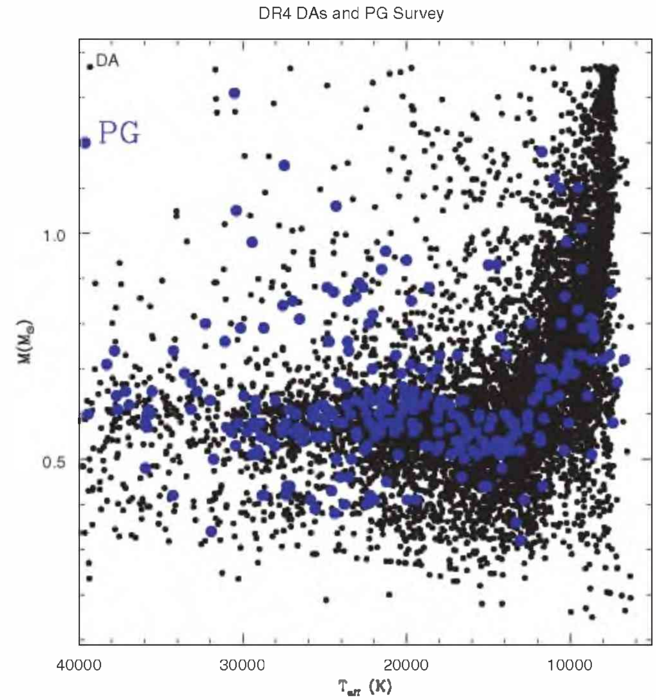

Figure 2. Masses for all 3595 DA white dwarf stars brighter than $g = 19$ and cooler than 40 000 K, showing an increase in mean mass for lower $T_{\rm eff}$. The large solid (blue) circles are the values published by Liebert et al. (2005), showing the increase in mass at lower $T_{\rm eff}$ is also present in their sample, which uses a totally independent grid of models and fitting technique.

complete sample of 348 DA stars with SNR $\geqslant$ 60 spectra and determined atmospheric parameters by spectral fitting via the line profile fitting technique, using models up to $\log g = 9.5$. They found a peak in the mass histogram at 0.565 $\mathcal{M}_\odot$ containing 75 per cent of the sample, a low-mass peak with 0.403 $\mathcal{M}_\odot$ containing 10 per cent of the sample, and a high-mass peak at 0.780 $\mathcal{M}_\odot$ containing 15 per cent of the stars. They fit their mass histogram (PG mass histogram from hereafter) with three Gaussian profiles: 0.565 $\mathcal{M}_\odot$ with $\sigma \simeq 0.080\,\mathcal{M}_\odot$, 0.403 $\mathcal{M}_\odot$ with $\sigma \simeq 0.023\,\mathcal{M}_\odot$ and a broad high-mass component at 0.780 $\mathcal{M}_\odot$ with $\sigma \simeq 0.108\,\mathcal{M}_\odot$. They found more stars above 1 $\mathcal{M}_\odot$ than can be described by the three Gaussians they fit. Marsh et al. (1997), Vennes et al. (1997) and Vennes (1999) also find an excess of white dwarf stars with masses above 1 $\mathcal{M}_\odot$ in their sample of $T_{\rm eff} > 23\,000$ K white dwarf stars.

The overall mass distribution of our bright sample matches well with that of the previous standard PG survey sample. We now explore the distribution with temperature.

In Fig. 2. we show the mass distribution versus temperature for DA stars brighter than $g = 19$ along with the similar distribution from Liebert et al. (2005). Again, we see the distributions are roughly equivalent and we see an increase in measured mass at lower temperatures. Our histograms use 0.025 $\mathcal{M}_\odot$ bins ($N/{\rm d}\,m$ = constant) because that is the approximately mean uncertainty in our mass determinations.

To explore the region of increasing mass further, Fig. 3 shows the mass histogram only for the 964 DAs brighter than $g = 19$, and $12\,000 \geqslant T_{\rm eff} \geqslant 8500$ K, for which we obtain $\langle \mathcal{M} \rangle_{\rm DA}^{\rm cool} \simeq 0.789 \pm 0.005\,\mathcal{M}_\odot$. We have excluded the stars cooler than $T_{\rm eff} = 8500$ K from our mass histograms because our cooler atmospheric models are not accurate for $\log g$ determination, as explained earlier.

Tables 1 and 2 detail the Gaussian fits we made for the histograms of Figs 1 and 3, respectively, with

$$N = \sum_i a_i \exp\left[-\frac{(\mathcal{M} - \mathcal{M}_i)^2}{2\sigma_i^2}\right]. \qquad (1)$$

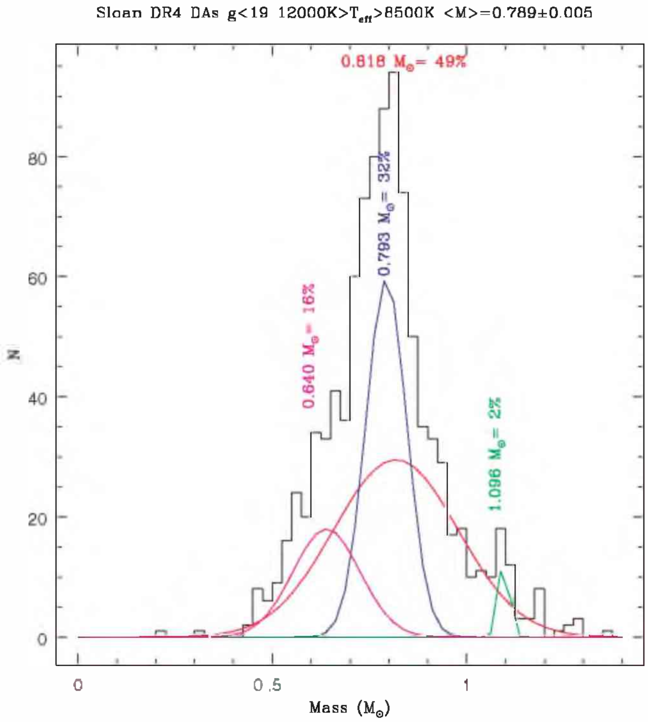

Figure 3. Histogram for the 964 DA stars brighter than $g = 19$, with $12\,000 \geqslant T_{\rm eff} \geqslant 8500$ K along with the fit Gaussians as detailed in Table 2.

Table 1. Gaussian fits for the $T_{\rm eff} \geqslant 12\,000$ K and $g \leqslant 19$ histogram, seen in Fig. 1.

i	a_i	$M_i(\mathcal{M}_\odot)$	σ_i	Fraction
1	264.8	0.578	0.047	69 per cent
2	27.8	0.658	0.149	23 per cent
3	27.0	0.381	0.050	7 per cent
4	3.0	1.081	0.143	1 per cent

Table 2. Gaussian fits for the 964 DAs with $12\,000 \geqslant T_{\rm eff} \geqslant 8500$ K and $g \leqslant 19$ histogram.

i	a_i	$M_i(\mathcal{M}_\odot)$	σ_i	Fraction
1	29.5	0.818	0.160	49 per cent
2	59.6	0.793	0.052	33 per cent
3	18.0	0.640	0.086	16 per cent
4	13.4	1.096	0.136	2 per cent

Fig. 11 of Liebert et al. (2005) also shows an increase in mass below $T_{\rm eff} = 12\,000$ K (see Fig. 2), even though they have a limited number of cooler stars due to colour selection effects in the PG survey. It is important to note that the model atmospheres used in Liebert et al. (2005) and the line profile fitting technique they use are totally independent of our own. Therefore, if the observed increase in the measured gravity with temperature is merely an artefact of the models, then similar problems must be present in two independent groups of models and fitting techniques. We are thus gathering increasing evidence that either (a) both DAs and DBs really do have higher mean masses at lower temperatures, or (b) there is a common artefact in the model used for all white dwarf spectral fitting.

4 WHY WE DO NOT TRUST MASSES FOR $T_{\rm eff} < 12\,000$ K FOR DA STARS

Bergeron et al. (1995) measured an increase in the mean mass for the ZZ Ceti star sample around $13\,000 > T_{\rm eff} > 11\,000$ K, but indicated it might come from a selection effect because the discovery of pulsating stars might have preferred higher mass stars. Arras, Townsley & Bildsten (2006) e.g. show that the white dwarf pulsators with lower masses should pulsate at cooler temperatures. Our sample of 351 bright stars in the same temperature range shows a similar increase in mass compared to the hotter sample, but we have not been biased by the pulsators, so an observational bias is not the cause for the increase in mass detected.

The simple expectation that massive stars cool faster than their less massive counterparts does not hold for $T_{\rm eff} \leqslant 10\,000$ K, as the most massive stars have smaller radius and, therefore, their cooling slows down after a few e-folding time-scales. Another possible explanation for an increased mean mass at lower effective temperatures is the presence of otherwise undetected He at the surface, broadening the observed H lines and thus mimicking a higher log g. Theoretical models (e.g. Fontaine & Wesemael 1991) indicate that only for DAs with hydrogen layer masses below $\mathcal{M}_{\rm H} = 10^{-10}\,\mathcal{M}_*$ will He mix around $T_{\rm eff} = 10\,000$ K and, if $\mathcal{M}_{\rm H} = 10^{-7}\,\mathcal{M}_*$, only below $T_{\rm eff} \simeq 6500$ K. However, all seismologically measured H layer masses are $\mathcal{M}_{\rm H} > 10^{-7}\,\mathcal{M}_*$ (Fontaine & Wesemael 1997; Bradley 1998, 2001, 2006). Since our increased mass trend happens significantly hotter than $T_{\rm eff} = 6500$ K, He contamination cannot account for the observed increase in mass at lower temperatures, unless the more distant stars studied here have significantly thinner H layers. Lawlor & MacDonald's (2006) models show around 3 per cent of the DAs could have $\mathcal{M}_{\rm H} \sim 10^{-9}\,\mathcal{M}_*$, but not thinner. Therefore, there are not enough stars with thin H layers, at any rate, to account for our excess of massive objects.

Wilson (2000) proposes a possible physical model for increasing white dwarf masses at lower temperatures. She suggests that low-metallicity AGB stars will produce higher mass white dwarf stars, probably around 1 $\mathcal{M}_\odot$, because the relatively lower mass loss expected for low metallicity AGB stars increases the mass of the core prior to the star moving out of the AGB. Since the earlier generations of white dwarf stars which have now cooled more than their later cohorts, presumably came from lower metallicity progenitors, this mechanism could explain a mass increase at lower white dwarf temperatures. If we extend this concept to globular clusters though, we would expect the mass of the white dwarfs in globular clusters to be larger than the mean mass of our stars cooler than 10 000 K, which is not observed (Moehler et al. 2004; Richer et al. 2006). So again, we are left with a discarded explanation of the observed mass increase.

An interesting clue to the problem may be found in Engelbrecht & Koester (2007), which used SDSS photometry alone to make a mass estimate. Their cool white dwarf stars show mean masses similar to those of the hotter stars. Our mass determination using photometric colours only, shown in Fig. 4, is derived comparing only the SDSS colours $(u - g)$ and $(g - r)$ with those predicted from the atmospheric models convolved with SDSS filters. They do not show any increase in mass with decreasing $T_{\rm eff}$. Because of their larger uncertainties than the spectra fitting, we binned the results in 2000-K bins. This result suggests that any problem in the models is mainly restricted to the line profiles, not the continua, which dominate the broad-band photometric colours.

Thus, we are mainly left with the possibility raised by Koester (1991) that an increase in mass with lower temperatures could be

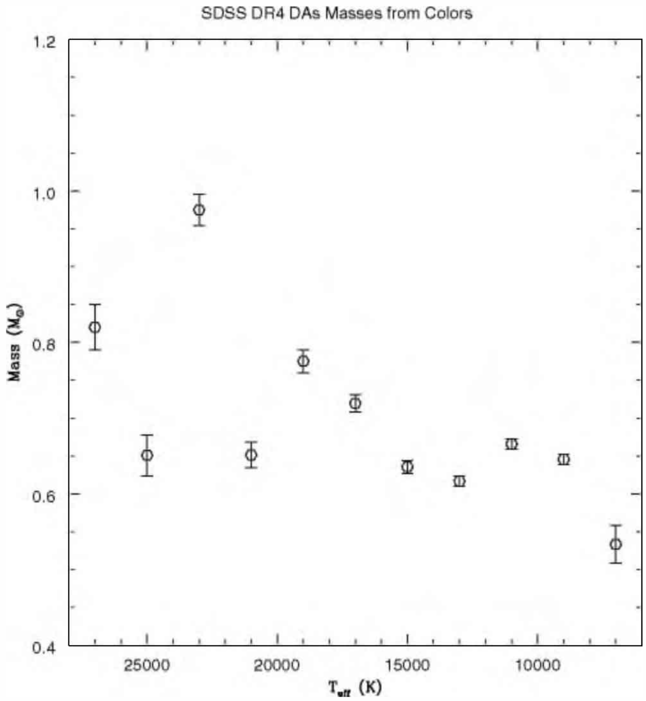

Figure 4. Masses for all 7167 DA white dwarf stars derived comparing only the SDSS colours $(u - g)$ and $(g - r)$ with those predicted from the atmospheric models. For $T_{\rm eff} \geqslant 20\,000$ K and $T_{\rm eff} \leqslant 9000$ K, the colours are degenerate in mass.

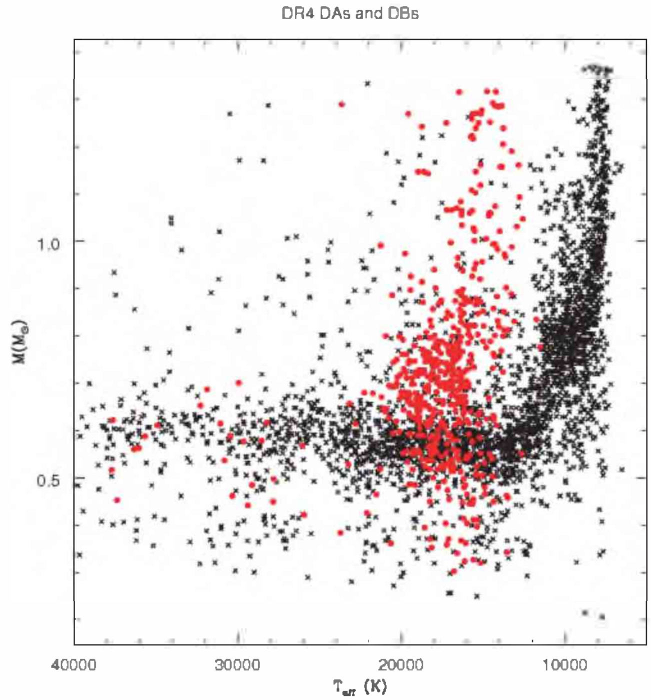

Figure 5. Masses for all 5718 DAs (crosses) cooler than 40 000 K and 507 DBs (filled circles) showing the continuous increase in average mass at lower $T_{\rm eff}$.

due to the treatment of neutral particles in model atmospheres with the Hummer–Mihalas formalism. Bergeron et al. (1995), however, suggest that the neutral particles are only important below $T_{\rm eff} \simeq 8000$ K which is certainly lower than where we see the trend begin. It seems the only remaining explanation is that accurate modelling of neutral particles will indeed show an effect for DAs near 12 000 K.

5 DB WHITE DWARFS

We determined masses for the Eisenstein et al. (2006) DBs from their fit temperatures and gravities using evolutionary grids of Althaus, Serenelli & Benvenuto (2001) and Althaus et al. (2005). The Althaus models use time resolved diffusion throughout evolution. Metcalfe (2005) and Metcalfe et al. (2005) discuss asteroseismological results in DBs, showing the observations are consistent with the layer masses predicted by current diffusion theory. Fig. 5 shows that we find an increase in the measured surface gravity below $T_{\rm eff} \simeq 12\,000$ K for DAs and a similar increase below $T_{\rm eff} \simeq 16\,000$ K for DBs. For the 208 DBs brighter than $g = 19$, we find $\langle \mathcal{M} \rangle_{\rm DB}^{\rm all} = 0.785 \pm 0.013\,\mathcal{M}_\odot$. For the 150 DBs brighter than $g = 19$ and hotter than $T_{\rm eff} = 16\,000$ K, we find $\langle \mathcal{M} \rangle_{\rm DB} = 0.711 \pm 0.009\,\mathcal{M}_\odot$. Both measurements are considerably larger than the 0.593 $\mathcal{M}_\odot$ mean mass value for the bright and hot DA sample. A similar larger (relative to that of the DAs) DB mean mass value has been previously reported by Koester et al. (2001) who obtained a $\langle \mathcal{M} \rangle_{\rm DB} = 0.77$ for the 18 DBs they observed with the Ultraviolet and Visual Echelle Spectrograph (UVES)/Very Large Telescope (VLT), including stars down to $T_{\rm eff} \sim 16\,000$ K. Others, however, find lower mean DB masses, more similar to those of the DAs. Oke, Weidemann & Koester (1984) derived $\langle \mathcal{M} \rangle_{\rm DB} = 0.55 \pm 0.10$ from their sample of 25 DBs ranging $30\,000 > T_{\rm eff} > 12\,000$ K, while Beauchamp (1995) found $\langle M \rangle_{\rm DB} = 0.59 \pm 0.01\,\mathcal{M}_\odot$ for his

Table 3. Gaussian fits for the histogram of the 150 DBs brighter than $g = 19$ and hotter than $T_{\rm eff} = 16\,000$ K.

i	a_i	$M_i(\mathcal{M}_\odot)$	σ_i	Fraction
1	8.3	0.700	0.109	59 per cent
2	14.3	0.712	0.042	40 per cent
3	0.6	1.288	0.035	1 per cent

46 DBs, ranging $12\,000 \geqslant T_{\rm eff} \geqslant 31\,000$ K. For the 34 DBs in Castanheira et al. (2006), ranging $27\,000 \geqslant T_{\rm eff} \geqslant 13\,000$ K, the mean is $\langle \mathcal{M} \rangle_{\rm DB} = 0.544 \pm 0.05\,\mathcal{M}_\odot$.

The Gaussian fits for the 153 DBs brighter than $g = 19$ and hotter than $T_{\rm eff} = 16\,000$ K are listed in Table 3. The mass histogram for DBs is shown in Fig. 6.

6 OBSERVING VOLUME CORRECTION

In order to turn our observed mass distributions into a real analytical tool, we must first correct the sample for completeness. We do this by the $1/V_{\rm max}$ formalism. $V_{\rm max}$ is the volume defined by the maximum distance at which a given object would still appear in a magnitude limited sample (Schmidt 1968). Geijo et al. (2006) discuss white dwarf luminosity function completeness corrections and conclude that for large samples, the $1/V_{\rm max}$ method provides a reliable characterization of the white dwarf luminosity function.

Liebert et al. (2005) find that 2.7 per cent of the stars in the PG sample have masses larger than 1 $\mathcal{M}_\odot$ and, when corrected by $1/V_{\rm max}$, 22 per cent are above 0.8 $\mathcal{M}_\odot$.

We first calculated each star's absolute magnitude from the $T_{\rm eff}$ and $\log g$ values obtained from our fits (for the extreme mass ones) or those of Eisenstein et al. (2006) (for the rest), convolving the synthetic spectra with the g filter transmission curve. We used the evolutionary models of Wood (1995) and Althaus et al. (2005) with

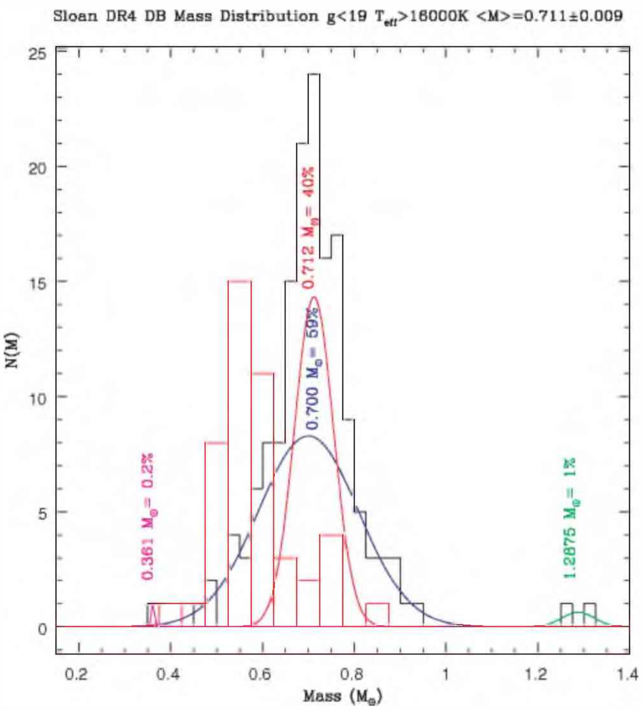

Figure 6. Histogram for the 150 DBs brighter than $g = 19$ and hotter than $T_{\rm eff} = 16\,000$ K in DR4.

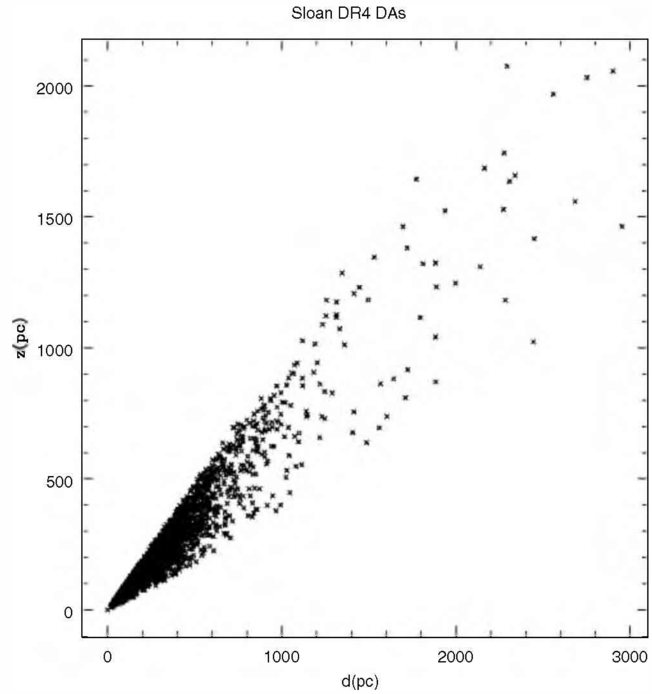

Figure 7. Distribution of distances, d, and height above the Galactic plane, z, for DAs in the SDSS DR4.

C/O cores up to $\log g = 9.0$, and O/Ne cores for higher gravities, $M_{\rm He} = 10^{-2} M_*$ and $M_{\rm H} = 10^{-4}$ or $0 M_*$, to estimate stellar radii for DAs and DBs, respectively. We do not claim that the SDSS spectroscopic sample is complete, but we do contend that in terms of mass, there should be no preferential bias in the target selection. Harris et al. (2006) report that spectra are obtained for essentially all white dwarf stars hotter than 22 000 K. Additional white dwarf stars down to $T_{\rm eff} = 8000$ K are also found, but few cooler than that as these stars overlap in colour space with the F, G and K main-sequence stars. Eisenstein et al. (2006) discuss the spectroscopic sample completeness, which is around 60 per cent at $18 < g < 19.5$ for stars hotter than $T_{\rm eff} = 12\,000$ K and around 40 per cent for cooler stars. Our analysis is restricted to the sample brighter than $g = 19$.

Once we had our calculated absolute magnitudes, we could estimate each star's distance as shown in Fig. 7, neglecting any effects of interstellar extinction. The mean distance for our DA samples are as follows: 474 ± 5 pc for the entire 7167 DA sample; 302 ± 5 pc for the stars brighter than $g = 19$ and 436 ± 7 pc for the stars brighter than $g = 19$ and hotter than $T_{\rm eff} \simeq 12\,000$ K.

For each star in our sample, we calculate

$$V_{\rm max} = \tfrac{4\pi}{3}\beta\left(r^3_{\rm max} - r^3_{\rm min}\right)\exp(-z/z_0),$$

where β is the fraction of the sky covered, 0.1159 for the DR4 sample, $r_{\rm min}$ is due to the bright magnitude limit, $g = 15$, and z_0 is the disc scaleheight which we assume to be 250 pc, as Liebert et al. (2005) and Harris et al. (2006), even though our height distribution indicates $z_0 \simeq 310$ pc. Vennes et al. (2005) show that both the white dwarf stars in the SDSS DR1, and the 1934 DAs found in the 2dF ($18.25 \leqslant b_J \leqslant 20.85$) quasar surveys, belong to the thin disc of our Galaxy. Using these data, they measured a scaleheight around 300 pc. Harris et al. (2006) calculate the white dwarf luminosity function from photometric measurements of the white dwarf stars discovered in the SDSS survey up to Data Release 3 (DR3). They assume $\log g = 8.0$ for all stars and use the change in number per

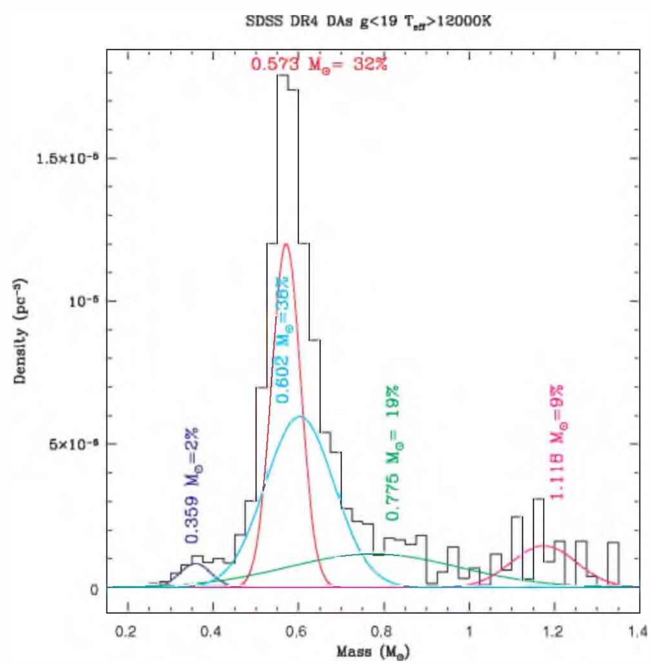

Figure 8. Histogram for the 1733 DA stars brighter than $g = 19$ ($V/V_{\rm max} \geqslant 0.45$) and hotter than $T_{\rm eff} = 12\,000$ K corrected by $1/V_{\rm max}$.

magnitude bin to calculate the scaleheight of the disc, obtaining 340^{+100}_{-70} pc, but adopt 250 pc for better comparison with other studies. This volume includes the disc scaleheight as discussed by Green (1980), Fleming, Liebert & Green (1986) and Liebert et al. (2005). Each star contributes $1/V_{\rm max}$ to the local space density.

Figs 8 and 9 show the resulting corrected mass distribution for our DA and DB sample, respectively. Fig. 8 contains 1733 bright,

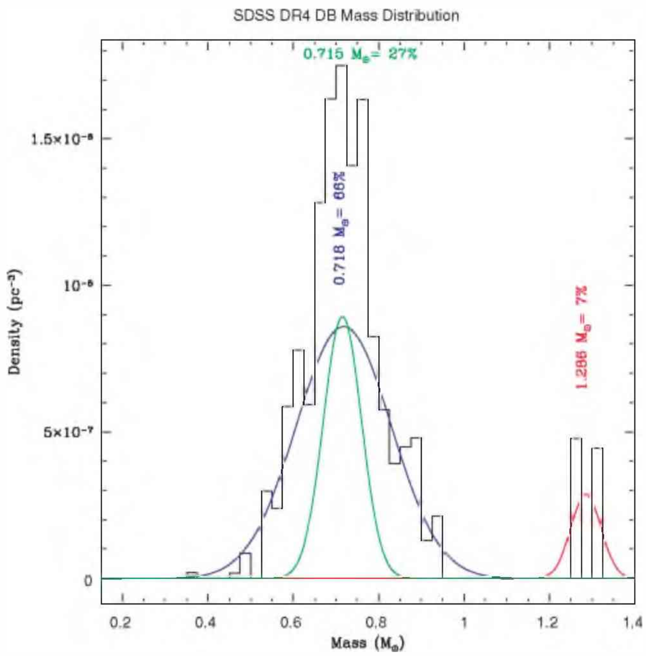

Figure 9. Histogram for the 150 DBs brighter than $g = 19$, and hotter than $T_{\rm eff} = 16\,000$ K in DR4, corrected by volume.

Table 4. Gaussian fits for the $T_{\rm eff} \geqslant 12\,000$ K and $g \leqslant 19$ volume corrected DA mass histogram.

i	a_i	$M_i(\mathcal{M}_\odot)$	σ_i	Fraction
1	5.965×10^{-6}	0.603	0.081	38 per cent
2	1.203×10^{-5}	0.571	0.034	32 per cent
3	1.165×10^{-6}	0.775	0.201	19 per cent
4	1.455×10^{-6}	1.175	0.076	9 per cent
5	8.305×10^{-7}	0.358	0.037	2 per cent

Table 5. Gaussian fits for the volume corrected histogram of the 150 DBs brighter than $g = 19$ and hotter than $T_{\rm eff} = 16\,000$ K.

i	a_i	$M_i(\mathcal{M}_\odot)$	σ_i	Fraction
1	8.6×10^{-7}	0.718	0.111	66 per cent
2	8.9×10^{-7}	0.715	0.045	27 per cent
3	2.9×10^{-7}	1.286	0.031	7 per cent

non-cool DAs, i.e. those with $T_{\rm eff} \geqslant 12\,000$ K and $g \leqslant 19$. We also list the corresponding five Gaussian fit parameters in Table 4. Fig. 9 contains 150 bright, non-cool DBs, i.e. those with $T_{\rm eff} \geqslant 16\,000$ K and $g \leqslant 19$. The corresponding three Gaussian fits are listed in Table 5.

Since the most massive white dwarf stars have smaller luminosities because of their smaller radii, after applying the $1/V_{\rm max}$ correction to the observed volume, we find that around 20 per cent DAs are more massive than $0.8\,\mathcal{M}_\odot$ in our bright and hot sample, of the same order as that discovered by Liebert et al. (2005) for the PG sample. The DB distribution is interesting, however, as it tends to significantly higher masses than does the DA distribution! We found only two stars from our sample with published atmospheric parameters in the literature, with $\Delta T_{\rm eff} = 510 \pm 30$ and $\Delta \log g = 0.12 \pm 0.15$, so we could not do a comparison as Kleinman et al. (2004) and Eisenstein et al. (2006) did for the DA results.

7 EXTREME MASS STARS

Nalężyty & Madej (2004) published a catalogue of all massive white dwarf stars then known, with 112 stars more massive than $0.8\,\mathcal{M}_\odot$. The four stars with $\mathcal{M} \geqslant 1.3\,\mathcal{M}_\odot$ in their list are magnetic ones and therefore have large uncertainties in their estimated masses. Dahn et al. (2004) found one non-magnetic massive white dwarf, LHS 4033, with $\mathcal{M} \simeq 1.318$–$1.335\,\mathcal{M}_\odot$, depending on the core composition. Our oxygen–neon core mass for their derived $T_{\rm eff} = 10\,900$ K and $\log g = 9.46$ is $\mathcal{M} \simeq 1.30\,\mathcal{M}_\odot$. We note that the models from the Montreal group used to derive $T_{\rm eff}$ and $\log g$ in Dahn et al. (2004) show the same increase in mass with decreasing $T_{\rm eff}$ as our models and therefore we do not take this mass determination as completely reliable due to the objects relatively low temperature. For GD 50 (WD J0348−0058), Dobbie et al. (2006) found $T_{\rm eff} = 41\,550 \pm 720$ K and $\log g = 9.15 \pm 0.05$. Our oxygen–neon core mass for their derived $T_{\rm eff}$ and $\log g$ is $\mathcal{M} \simeq 1.23 \pm 0.02\,\mathcal{M}_\odot$, very similar to the value reported by them for C/O models. They also show this massive star is consistent with its formation and evolution as a single star, not the product of a merger.

From the 7755 pure DA white dwarf stars, we found 1611 (22 per cent) with $\mathcal{M} > 0.8\,\mathcal{M}_\odot$. For the 2945 stars brighter than $g = 19$ we found 760 (26 per cent) with $\mathcal{M} > 0.8\,\mathcal{M}_\odot$, but for the 1733 stars brighter than $g = 19$ and hotter than $T_{\rm eff} = 12\,000$ K, we find only 105 stars (6 per cent) with $\mathcal{M} > 0.8\,\mathcal{M}_\odot$. The most massive star in our hot and bright sample is SDSS J075916.53+433518.9, whose spectrum spSpec-51883-0436-045 is shown in Fig. 10, with $g = 18.73$, $T_{\rm eff} = 22100 \pm 450$ K, $\log\ g = 9.62 \pm 0.07$, $\mathcal{M} = 1.33 \pm 0.01\,\mathcal{M}_\odot$ and estimated distance of $d = 104 \pm 4$ pc. We caution that

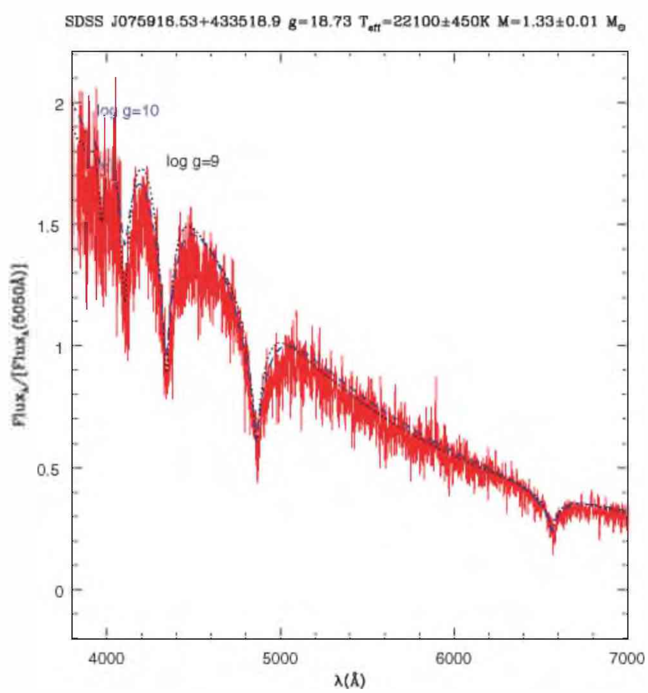

Figure 10. Spectrum of SDSS J075916.53+433518.9 with $g = 18.73$, $T_{\rm eff} = 22\,100$ K and two models, with $\log g = 9$ and 10. The higher $\log g$ fits the Hα line better, but the lower $\log g$ fits the higher lines better, where the SNR is smaller. This low SNR is typical for the stars closer to our upper cut-off of $g = 19$.

Table 6. DA stars with masses above 1.2 $\mathcal{M}_\odot$ and below 1.3 $\mathcal{M}_\odot$ derived from the SDSS spectra, with $T_{\rm eff} \geqslant 12\,000$ K.

Spectra-M-P-F	Name	g	M_g	$T_{\rm eff}$ (K)	σ_T (K)	$\log g$	σ_g	$\mathcal{M}$ ($\mathcal{M}_\odot$)	σ_M ($\mathcal{M}_\odot$)	d (pc)
spSpec-51691-0342-639	SDSS J155238.21+003910.3	18.44	12.23	15 924	387	9.280	0.050	1.262	0.010	97
spSpec-51915-0453-540	SDSS J094655.94+600623.4	17.99	10.87	28 125	220	9.370	0.040	1.287	0.010	123
spSpec-52374-0853-198	SDSS J133420.97+041751.1	18.52	12.34	17 549	422	9.150	0.060	1.223	0.020	125
spSpec-52703-1165-306	SDSS J150409.88+513729.1	18.84	10.28	79 873	8228	9.050	0.390	1.204	0.100	468
spSpec-52751-1221-177	SDSS J110735.32+085924.5	18.42	12.23	18 715	327	9.140	0.060	1.219	0.020	128
spSpec-52872-1402-145	SDSS J154305.67+343223.6	18.33	10.85	30 472	313	9.300	0.070	1.269	0.010	168

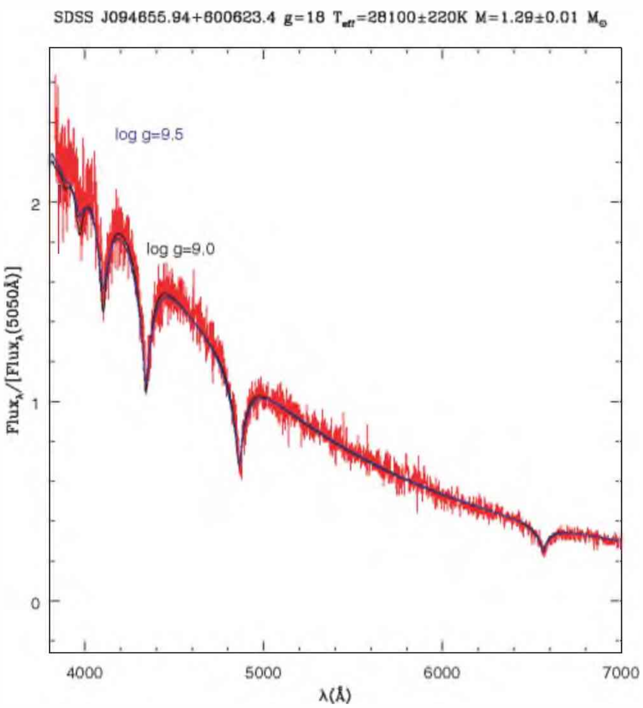

Figure 11. Spectrum of SDSS J094655.94+600623.4 with $g = 17.99$, $T_{\rm eff} = 28\,100$ K and two models, with $\log g = 9$ and 9.5. This spectrum is typical of the SNR achieved for the 1003 DAs and 59 DBs brighter than $g = 18$ in our sample.

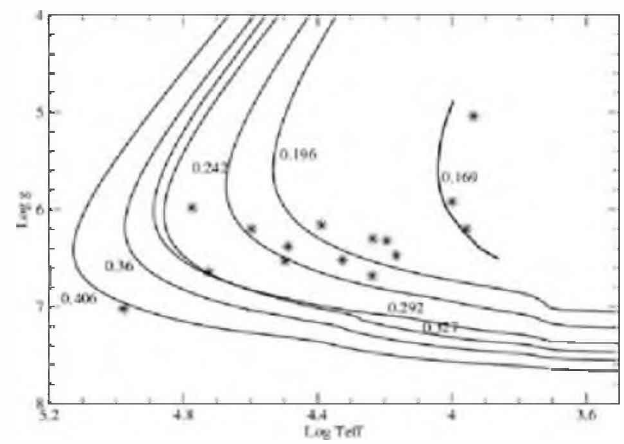

Figure 12. Evolutionary tracks for He white dwarf stars calculated by Althaus et al. (2001) and the location of the lowest mass stars in our sample. Most of these stars are below $g = 19$ and therefore have noisy spectra.

the evolutionary models used to estimate the radii, and therefore the masses, in our analysis do not include post-Newtonian corrections, important for masses above $\mathcal{M} \simeq 1.30\,\mathcal{M}_\odot$ (Chandrasekhar & Tooper 1964). For the stars brighter than $g = 19$, we find 21 others with masses larger than $\mathcal{M} = 1.3\,\mathcal{M}_\odot$, all below $T_{\rm eff} = 9000$ K. We deem the mass determinations for stars cooler than $T_{\rm eff} \simeq 12\,000$ K unreliable. In Table 6, we list the DAs with $1.2 < \mathcal{M} < 1.3\,\mathcal{M}_\odot$ hotter than $T_{\rm eff} = 12\,000$ K.

The spectrum for the brighter $g = 17.99$ SDSS J094655.94+600623.4 is shown in Fig. 11. Because our analysis uses relatively low SNR spectra and gravity effects dominate mainly below 3800 Å, where we have no data, our conclusion is that we must undertake a study in the violet or ultraviolet to measure the masses more accurately. An extensive study of gravitational redshift would also be critical.

For the 507 single DBs we find 30 DBs with $\log g > 9$. Most of our massive DBs are cooler than $T_{\rm eff} \simeq 16\,000$ K, or fainter than $g = 19$, except for SDSS J213103.39+105956.1 with $g = 18.80$, $T_{\rm eff} = 16\,476 \pm 382$ and $\log g = 9.64 \pm 0.21$, corresponding to a mass $\mathcal{M} = 1.33 \pm 0.04\,\mathcal{M}_\odot$, and for SDSS J224027.11−005945.5 with $g = 18.82$, $T_{\rm eff} = 17\,260 \pm 402$, and $\log g = 9.31 \pm 0.20$, corresponding to a mass $\mathcal{M} = 1.25 \pm 0.06\,\mathcal{M}_\odot$.

The low-mass stars present in our sample are consistent with He core evolution models calculated by Althaus et al. (2001), and displayed in Fig. 12. It is important to stress that these stars should be studied with more accurate spectra and model atmospheres, as they are possible progenitors of Type Ia supernova if they accrete mass from companions.

8 CONCLUSIONS

Our investigations into the mass distribution of the SDSS DR4 white dwarf sample from Eisenstein et al. (2006) revealed several items. First, all groups are seeing nearly identical increases in mean DA at lower temperatures (less than $\approx$12 000 K for DAs and 16 000 K for DBs). Either this is truly going on in the white dwarf stars, or there is missing or incorrect physics in everyone's models. We propose the treatment of neutral particles as the most likely explanation. We suspect the atmospheric models should be improved with a detailed inclusion of the line broadening by neutral particles, since the increase in apparent mass for both DAs and DBs occur at temperatures when recombination becomes important.

Secondly, we find a significant difference between the DA and DB mass distributions, with the DB distribution significantly more weighted to massive stars. Figs 13 and 14 show the combined DA and DB histograms. The DB histograms have been renormalized to the DA maximum for display purposes. Our results contradict

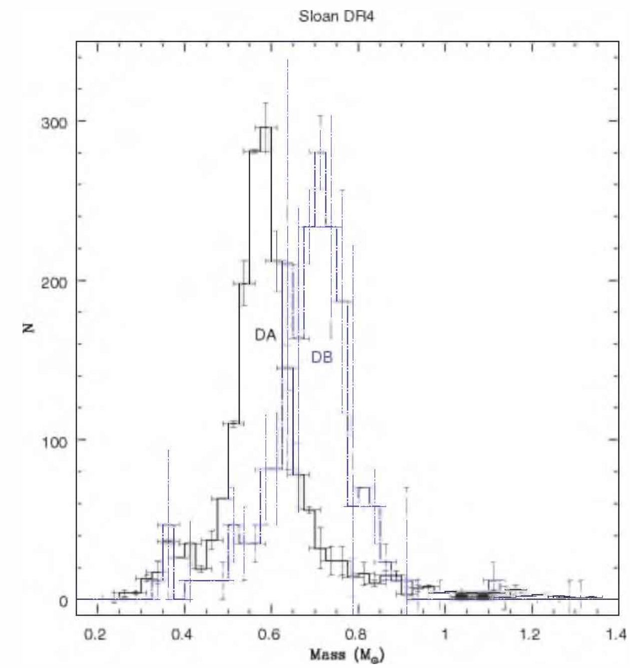

Figure 13. DA and DB histograms for comparison. The DB histogram has been renormalized to the DA maximum for display purposes.

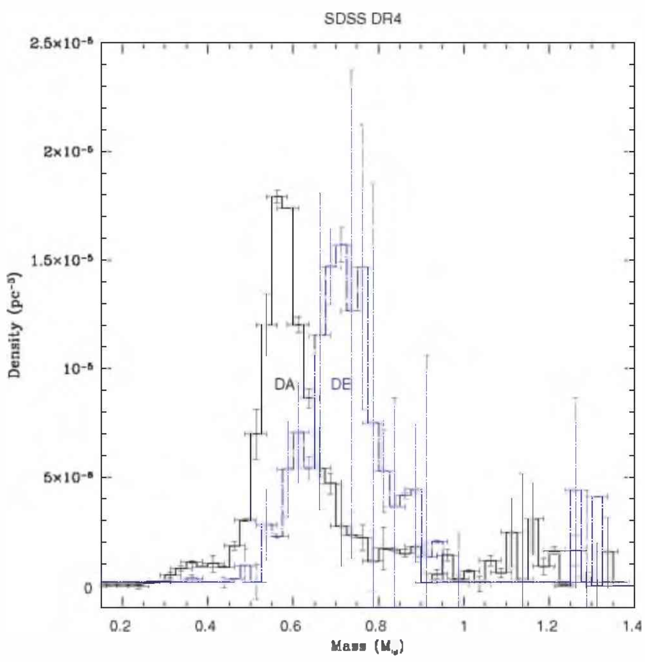

Figure 14. DA and DB histograms corrected by observed volume for comparison. The DB histogram has been renormalized to the DA maximum for display.

nearly all previous work which show the mean DA and DB masses to be similar (with the exception of Koester et al. 2001). We note that the previous efforts, though, were based on histograms for DBs with less than 50 stars, and our DB histogram has 150 stars. However, we still need to explore our DB models and fits in more detail to verify the validity of this novel result. Specifically, we find $\langle \mathcal{M} \rangle_{\rm DB} = 0.711 \pm 0.009\, \mathcal{M}_\odot$, higher than $\langle \mathcal{M} \rangle_{\rm DA} = 0.593 \pm 0.016\, \mathcal{M}_\odot$ for the 1733 DAs brighter than $g = 19$, and hotter than $T_{\rm eff} = 12\,000$ K. This is a significant new result and must be investigated further.

We have also detected a large number of massive DA white dwarf stars: 760 with $\mathcal{M} > 0.8\,\mathcal{M}_\odot$ brighter than $g = 19$ and 105 both brighter than $g = 19$ and hotter than $T_{\rm eff} = 12\,000$ K. We report the highest log g white dwarf ever detected.

ACKNOWLEDGMENTS

We thank Dr Daniel Eisenstein for some helpful suggestions, and his AUTOFIT code, and the referee, Dr Martin Barstow, for very detailed and useful comments that improved the presentation of the paper.

REFERENCES

Althaus L. G., Serenelli A. M., Benvenuto O. G., 2001, MNRAS, 323, 471
Althaus L. G., García-Berro E., Isern J., Córsico A. H., 2005, A&A, 441, 689
Arras P., Townsley D. M., Bildsten L., 2006, ApJ, 643, L119
Beauchamp A., 1995, PhD thesis, Univ. Montreal
Bergeron P., Wesemael F., Fontaine G., 1991, ApJ, 367, 253
Bergeron P., Wesemael F., Lamontagne R., Fontaine G., Saffer R. A., Allard N. F., 1995, ApJ, 449, 258
Bohm K. H., Cassinelli J., 1971, A&A, 12, 21
Bradley P. A., 1998, ApJS, 116, 307
Bradley P. A., 2001, ApJ, 552, 326
Bradley P. A., 2006, Mem. Soc. Astron. Ital., 77, 437
Castanheira B. G., Kepler S. O., Handler G., Koester D., 2006, A&A, 450, 331
Chandrasekhar S., Tooper R. F., 1964, ApJ, 139, 1396
Dahn C. C., Bergeron P., Liebert J., Harris H. C., Canzian B., Leggett S. K., Boudreault S., 2004, ApJ, 605, 400
Dobbie P. D., Napiwotzki R., Lodieu N., Burleigh M. R., Barstow M. A., Jameson R. F., 2006, MNRAS, 373, L45
Eisenstein D. J. et al., 2006, ApJS, 167, 40
Engelbrecht A., Koester D., 2007, in Napiwotzki R., Barstow M., eds, 15th European White Dwarf Workshop. APS, in press
Finley D. S., Koester D., Basri G., 1997, ApJ, 488, 375
Fleming T. A., Liebert J., Green R. F., 1986, ApJ, 308, 176
Fontaine G., Wesemael F., 1991, in Michaud G., Tutukov A., eds, Proc. IAU Symp. 145, Evolution of the Stars: the Photospheric Abundance Connection. Kluwer, Dordrecht, p. 421
Fontaine G., Wesemael F., 1997, in Isern J., Hernanz M., Garcia-Berro E., eds, Astrophys. Space Sci. Library Vol. 214, White Dwarfs, Proc. 10th European Workshop on White Dwarfs. Kluwer, Dordrecht, p. 173
Geijo E. M., Torres S., Isern J., García-Berro E., 2006, MNRAS, 369, 1654
Green R. F., 1980, ApJ, 238, 685
Harris H. C. et al., 2006, AJ, 131, 571
Kepler S. O., Castanheira B. G., Saraiva M. F. O., Nitta A., Kleinman S. J., Mullally F., Winget D. E., Eisenstein D. J., 2005, A&A, 442, 629
Kepler S. O., Castanheira B. G., Costa A. F. M., Koester D., 2006, MNRAS, 372, 1799
Kleinman S. J. et al., 2004, ApJ, 607, 426
Koester D., 1991, in Vauclair G., Sion E. M., eds, Proc. 7th European Workshop on White Dwarfs, NATO ASI Ser. Kluwer, Dordrecht, p. 343
Koester D. et al., 2001, A&A, 378, 556
Lawlor T. M., MacDonald J., 2006, MNRAS, 371, 263
Lemke M., 1997, A&AS, 122, 285
Liebert J., Bergeron P., Holberg J. B., 2005, ApJS, 156, 47
McCook G. P., Sion E. M., 2003, VizieR Online Data Cat., 3235, 1
Madej J., Należyty M., Althaus L. G., 2004, A&A, 419, L5
Marsh M. C. et al., 1997, MNRAS, 286, 369
Metcalfe T. S., 2005, MNRAS, 363, L86
Metcalfe T. S., Nather R. E., Watson T. K., Kim S.-L., Park B.-G., Handler G., 2005, A&A, 435, 649

Moehler S., Koester D., Zoccali M., Ferraro F. R., Heber U., Napiwotzki R., Renzini A., 2004, A&A, 420, 515
Należyty M., Madej J., 2004, A&A, 420, 507
Napiwotzki R., Green P. J., Saffer R. A., 1999, ApJ, 517, 399
Oke J. B., Weidemann V., Koester D., 1984, ApJ, 281, 276
Richer H. B. et al., 2006, in Napiwotzki R., Barstow M., eds, 15th European White Dwarf Workshop. APS, in press
Schmidt M., 1968, ApJ, 151, 393
Vennes S., 1999, ApJ, 525, 995
Vennes S., Thejll P. A., Galvan R. G., Dupuis J., 1997, ApJ, 480, 714
Vennes S. et al., 2005, in Shipman H. L., Sion E. M., Vennes S., eds, White Dwarfs as Cosmological and Galactic Probes. Kluwer, Dordrecht, p. 49
Wilson L. A., 2000, ARA&A, 38, 573
Wood M. A., 1995, in Koester D., Werner K., eds, LNP Vol. 443, White Dwarfs. Springer-Verlag, Berlin, p. 41
York D. G. et al., 2000, AJ, 120, 1579

This paper has been typeset from a TEX/LATEX file prepared by the author.